Single-cell-based sensors and synchrotron FTIR spectroscopy: A hybrid system towards bacterial detection

Mandana Veiseh [a], Omid Veiseh [a], Michael C. Martin [b],
Carolyn Bertozzi [c], Miqin Zhang [a,*]

[a] *Department of Materials Science & Engineering, University of Washington, United States*
[b] *Advanced Light Source Division, Lawrence Berkeley National Laboratory, United States*
[c] *Department of Chemistry, University of California at Berkeley, United States*

Abstract

Microarrays of single macrophage cell-based sensors were developed and demonstrated for potential real-time bacterium detection by synchrotron FTIR microscopy. The cells were patterned on gold electrodes of silicon oxide substrates by a surface engineering technique, in which the gold electrodes were immobilized with fibronectin to mediate cell adhesion and the silicon oxide background was passivated with polyethylene glycol (PEG) to resist protein adsorption and cell adhesion. Cell morphology and IR spectra of single, double, and triple cells on gold electrodes exposed to lipopolysaccharide (LPS) of different concentrations were compared to reveal the detection capability of this cell-based sensing platform. The single-cell-based system was found to generate the most significant and consistent IR spectrum shifts upon exposure to LPS, thus providing the highest detection sensitivity. Changes in cell morphology and IR shifts upon cell exposure to LPS were found to be dependent on the LPS concentration and exposure time, which established a method for the identification of LPS concentration and infected cell population. Possibility of using this single-cell system with conventional IR spectroscopy as well as its limitation was investigated by comparing IR spectra of single-cell arrays with gold electrode surface areas of 25, 100, and 400 μm^2 using both synchrotron and conventional FTIR spectromicroscopes. This cell-based platform may potentially provide real-time, label-free, and rapid bacterial detection, and allow for high-throughput statistical analyses, and portability.
© 2007 Elsevier B.V. All rights reserved.

Keywords: Biosensors; Cell adhesion; FTIR; BioMEMS; Cell-based sensors

1. Introduction

Study of single cell behavior in a specified chemical or biological environment holds important implication in cell biology, biochemistry, and development of cell-based sensors, as it reveals a spectrum of responses from each individual cell under stimulation (Chiou et al., 2005). In a multi-cell system, critical information may be lost or submerged in averaged bulk cell measurements (Teruel and Meyer, 2002). Particularly, in a cell-based sensor array, the signal generated by a multi-cell sensing element in response to an analyte is embedded with the interferential signals (noises) resulted from cell–cell interactions in the cell cluster. Furthermore, variations in conformation of cell clusters on multi-cell electrodes of any array may result in a different response even when they host similar number of cells. Thus, reducing or eliminating the interference from cell–cell interactions represents a major challenge in development of cell-based sensors.

Cell-based sensors are hybrid systems (biology + device) that use cells' remarkable abilities to detect, transduce, and amplify very small changes of external stimuli (Lorenzelli et al., 2003). They offer new opportunities for many biomedical applications, including biothreat detection, drug evaluation, pollutant identification, and cell type determination (Bashir, 2004). They are generally constructed by interfacing cells to a transducer that converts cellular responses into signals detectable by electronic

---

* Corresponding author at: Department of Materials Science & Engineering, University of Washington, 302L Roberts Hall, Seattle, WA 98195-2120, United States. Tel.: +1 206 616 9356; fax: +1 206 543 3100.

E-mail address: mzhang@u.washington.edu (M. Zhang).

or optical devices. Recent years have witnessed a substantial growth in application of planar microelectrode arrays in cell-based biosensors (CBBs) (van Bergen et al., 2003; Wang and Li, 2003; Yang et al., 2003), because they can be easily interfaced with electronic, optical or chemical detecting mechanisms (Miller et al., 2002). Major advantages of these sensing arrays over conventional biosensors include rapid and inexpensive analyses, much smaller sample size requirement, low sample contamination, high throughput and sensitivity, and portability. Among cell-based sensors, single-cell-based sensors are of particular interest; with an array of virtually identical single cells as sensing elements integrated with real-time data acquisition technology, it is possible to experimentally study cellular pathways without interference from other cells, thereby eliminating the uncertainty incurred by states of neighboring cells (Elowitz et al., 2002). Statistical analysis of cell behavior, a topic extensively pursued in cell biology, requires closely identical cell sites (Hyden, 1995), and a single-cell-based system may ideally serve the purpose.

In this study, a cell-based sensor platform was established by combining a microarray of single macrophage cells with synchrotron FTIR spectromicroscopy for real-time potential bacterial detection, and its sensing capability was demonstrated through a comparison study with multi-cell sensor systems. Using a previously established technology (Veiseh and Zhang, 2006) silicon oxide substrates were patterned with an array of gold square electrodes and surface modified to host a single or a group of macrophage cells. Conventional technologies for detection and identification of bacteria, including immunoassay, genetic markers, and cell culturing, use reagent-based tools, which are slow and/or costly due to their reliance on expensive consumables. For example, *Salmonella* detection takes 3–4 days for presumptive results and another 5–7 days for confirmation (Andrews, 1992). The technique introduced in this study may potentially allow for rapid detection of bacteria in a few hours. Lipopolysaccharide (LPS) was used as our model analyte in view of its effects on macrophages. LPS is a major structural component of gram-negative bacterial cell wall and a potent activator of the macrophage cells. LPS is also a major pathogenic factor causing septic shock syndrome and death in critically ill patients (Cohen, 2002; Fujihara et al., 2003; Raetz, 1990; Ulevitch and Tobias, 1995). The syndrome is primarily caused by an overproduction of pro-inflammatory cytokines after macrophage cells have been activated by lipopolysaccharide (Akashi et al., 2000; Kirkley et al., 2003; Rovida et al., 2001; Schumann et al., 1990; Soler et al., 2001; Triantafilou and Triantafilou, 2003; Zhang et al., 1997). Macrophage activation by LPS and its products are both dose-dependent and heterogeneous (Frevel et al., 2003; Hamilton et al., 1986; Wiklund et al., 1999). Using synchrotron IR spectroscopy and DIC reflectance imaging we investigated and compared LPS-induced responses of cells in isolated (single cell) and communicating (colony of the cells) states. To illustrate how the light source quality would affect sensitivity and spatial resolution of the cell-based sensors, the spectra generated by the synchrotron was compared with those generated by a conventional FTIR source.

2. Experimental

2.1. Materials

The following materials and chemicals were used as received: silicon wafers of (1 0 0) orientation (Wafernet, CA), Nanostrip 2× (Cyantek, Fremont, CA), 11-mercaptoundecanoic acid 95% (11-MUA), 3-mercaptopropionic acid 99% (3-MPA), N-hydroxysuccinimide 97% (NHS), 1-ethyl-3-(3-dimethylamino-propyl) carbodiimide (EDAC) (Sigma, St. Louis, MO), 2-[methoxy(polyethyleneoxy)propyl] trimethoxysilane (M_w = 460–590 Da) (Gelest, Morrisville, PA), fibronectin protein, Trypsin–EDTA, Sigmacote and lipopolysaccharide (*E.-coli* 0111:B4, endotoxin unit: 500,000) (Sigma, Milwaukee, WI). Nanostrip 2× was purchased from Gelest (Morrisville, PA). All the solvents including toluene, triethylamine, and dimethylformamide were purchased from Aldrich (Milwaukee, WI). Absolute ethanol was always deoxygenated by dry N_2 before use. RAW264.7 cells (murine monocyte/macrophage) were purchased from American Type Culture Collection (Manassas, VA). The following cell culture reagents were purchased from Gibco (Carlsbad, CA): Trypan Blue, Fetal Bovine Serum, HBSS (Hanks balanced Salt Solution), DMEM (Dulbecco's modified Eagle's medium with 4 mM L-glutamine adjusted to contain 1.5 g/L sodium bicarbonate and 4.5 g/L glucose).

2.2. Substrate preparation

The 4″ p-type silicon substrates of (1 0 0) orientation were cleaned with piranha (hydrogen peroxide/sulfuric acid 2:5, v/v) at 120 °C for 10 min, dipped in HF, and thoroughly rinsed with DI water. A layer (1.1 μm) of positive photoresist was then coated on the surface, and patterns were formed on the substrate upon exposure to ultraviolet light through a mask with square patterns of three different sizes (25, 100, and 400 μm²). A titanium (Ti) layer (10 nm) was then deposited on the photoresist-developed substrates at a deposition rate of 0.3 Å/s. A gold film of 100 nm thickness was subsequently deposited on the Ti at a deposition rate of 5 Å/s. The photoresist was dissolved in acetone and the remaining metal film was lifted off. After lift off, the surface was exposed to buffered oxide etch (HF/NH4F 5:1, v/v) for 60 s and rinsed with DI water to remove native oxide on silicon before oxidation. The surface oxidation was performed under a dry oxygen flow for 6 h at 400 °C. The gold-patterned silicon oxide substrates were then cut into slides of 8 mm × 8 mm. To prevent surface contamination and scratches, the silicon oxide wafers were coated with a 2 μm layer of photoresist on their polished sides before cutting.

2.3. Surface modification

The surface was modified following a previously established procedure with minor modifications (Lan et al., 2005; Veiseh et al., 2002; Veiseh and Zhang, 2006). The protective photoresist layer on gold-patterned silicon substrates was removed by sonication for 10 min in acetone, 2 min in ethanol, and 2 min

in DI water. The substrates were then placed in Nanostrip 2× solution (H_2SO_5) at room temperature for 20 min, and dried under nitrogen, resulting in a hydroxyl layer on the silicon oxide surface.

The gold electrodes on the substrate were first reacted with a 20 mM mixture of alkane thiols of 11-mercaptoundecanoic acid (MUA) and 3-mercaptopropionic acid (MPA) (1:10, v/v) for 16 h to create a self-assembled monolayer (SAM). The silicon oxide background was passivated with polyethylene glycol (PEG). The PEG solution was prepared in a nitrogen-filled reaction flask by adding 3 mM methoxy-PEG-silane in deoxygenated toluene containing 1% triethylamine as catalyst. The Nanostrip-treated substrate was then placed in a separate nitrogen-filled flask that was rendered hydrophobic with Sigmacote to minimize the side reaction of PEG with the flask. The PEG reaction proceeded under nitrogen at 60 °C for 18 h. Physically adsorbed moieties were removed from the PEG-treated surface by sonication in toluene and ethanol for 5 min each, followed by rinsing with DI water and drying under nitrogen. The substrate with alkane thiol SAM on gold and M-PEG-silane on the silicon oxide background was immersed in an aqueous solution of 150 mM EDAC and 30 mM *N*-hydroxysuccinimide (NHS) for 30 min to attach the NHS group to the –COOH terminus of SAM. The substrate with NHS on gold and PEG on silicon oxide was sterilized with 70% ethanol for 15 min, and exposed to fibronectin protein at a concentration of 0.05 mg/mL in a phosphate buffer solution (PBS) of pH 8.2 at room temperature for 45 min. To remove loosely bound moieties from the surface after each step of the surface modification, the substrate was rinsed with the original solvent and then DI water.

2.4. Cell culture

RAW264.7 of passage less than 10 was cultured at 37 °C in a 5% CO_2-humidified incubator and grown in DMEM medium supplemented with 10% (v/v) heat-inactivated FBS, 4 mM L-glutamine, 1.5 g/L sodium bicarbonate, 4.5 g/L glucose, 100 units/mL penicillin, and 100 g/mL streptomycin. Cells were subcultured by a cell scrapper once a week. Culture conditions were the same for both LPS treated and control cells on surfaces. LPS treatments were performed using a stock solution of lipopolysaccharide (500,000 endotoxin units/mg) from *E. coli* 0111:B4 in HBSS at 1 mg/mL. RAW264.7 cells at a concentration of 2.5×10^5 cells/mL in DMEM medium were exposed to LPS at doses of 0.1, 1, or 10 µg/mL, and 0.5 mL of solutions were incubated with the surfaces for up to 21 h under sterile condition to avoid contamination.

2.5. Cell viability assay

After cell culture, both LPS treated and un-treated (control) cell-patterned substrates were washed twice with PBS and placed in 500 µL of Annexin V binding buffer (10 mM HEPES, 140 mM NaCl, 2.5 mM $CaCl_2$, pH 7.4). The substrates were incubated with a mixture of 100 µl of Annexin V and 2 µl of propidium iodide solutions for 15 min at room temperature, washed twice with the binding buffer, and visualized with a fluores-

cence microscope. The green fluorescently labeled Annexin V protein (in the presence of calcium) specifically binds to the phosphatidylserine protein on membranes of apoptotic cells. Propidium iodide does not penetrate either live or apoptotic cells, but stains nuclei of necrotic cells in red.

2.6. Differential interference contrast (DIC) reflectance microscopy

Cell-cultured surfaces were examined with a differential interference contrast (DIC) reflectance microscope (Nikon E800 Upright Microscope, NY, NY) equiped with DIC-20× (N.A. 0.46) and DIC-50× (N.A. 0.8) objectives. Images were acquired with a Coolsnap camera (series A99G81021, Roper scientific Inc., AZ, USA) attached to the microscope and a computer.

2.7. FTIR spectromicroscopy of cells on patterned substrates

IR spectra and optical reflectance DIC images were acquired from cells on the patterned substrates with single or a group of macrophage cells on each electrode both before and after cellular exposure to LPS. Synchrotron FTIR spectra were acquired from cell-patterned surfaces with a Nicolet Magna 760 FTIR bench and a Nicolet Nic-Plan™ IR microscope equipped with a computer-controlled *x–y–z* sample stage (via Nicolet Atlµs™ and OMNIC software) and an MCT-A detector at Beamline 1.4.3 of the Advanced Light Source (ALS) in Lawrence Berkeley National Laboratory, Berkeley CA (Martin and McKinney, 1998, 2001). In order to align the incident IR beam onto the substrate, an IR map (with 2–10 µm step size in *x–y* plane) was acquired around a gold electrode for a full IR range of 400–10,000 wave numbers. Under this condition the whole spectrum appeared as a broad peak and an intensity profile was given for the mapped region. The *x*, *y* positions were adjusted so that the highest intensity region of the beam was aligned with the center of the gold electrode. The samples were measured at wave numbers of 650–10,000 cm^{-1} using an XT-KBr beamsplitter and a MCT detector. The synchrotron infrared light is focused to a diffraction-limited spot size with a wavelength-dependent diameter of approximately 3–10 µm across the mid-IR range of interest (Carr, 2001; Dumas et al., 2004; Levinson et al., 2006). An on-stage temperature controlled mini incubator was used to maintain a proper environment for cellular analysis. Prior to infrared analysis, dead and loosely bound cells were removed from the substrate by three PBS washes (to eliminate the possible interference of dead and loosely bound cells to the real-time signals generated by live cells), the cell culture medium was replaced with fresh sterile medium, and the substrate covered with a layer of the medium was transferred to the mini incubator. The spectra were acquired in less than 10 min following the sample transfer to ensure cell viability and to minimize possible interference from environmental changes. Synchrotron FTIR spectra of 128 scans at a resolution of 8 cm^{-1} were acquired from individual electrodes patterned with cells. Background signals were collected from the silicon oxide surface of the same substrate right before the data collection. Images of 75 elec-

trodes were captured and signals from four electrodes hosting cells of similar morphologies were collected and averaged for each type of LPS treatment. All spectra were baseline-corrected and normalized to account for the continuous decay of the synchrotron beam in the storage ring. An appropriately scaled water vapor spectrum was subtracted from the spectra of cells. The spectra obtained with conventional FTIR were acquired from cell-patterned surfaces using a Thermo-Electron Nexus 870 bench and a Thermo-Electron Continuum infrared microscope with an MCT-A detector at Beamline 1.4.4 of the ALS under the same conditions set for the synchrotron measurements, except that an aperture size of 90 μm × 90 μm were employed to maximize the signal intensity.

3. Results and discussion

The process of surface modification for cellular attachment on gold microelectrodes on a silicon oxide substrate is illustrated in supplementary Fig. 1. Each gold microelectrode is activated with an alkane thiol self-assembled monolayer (SAM) and is covalently reacted with a cell adhesive protein (fibronectin) through an *N*-hydroxysuccinimide (NHS) coupling agent.

The silicon oxide regions are passivated with methoxy-polyethylene glycol-silane as reported previously (Veiseh and Zhang, 2006). In this platform each microelectrode hosts one to three cells depending on electrode size and cell concentration in culture. Patterning cells on a microarray conforms to the MEMs infrastructure and provides an easy way to accurately position cells. This eliminates the cumbersome process of finding the cells that have a similar size before each experiment, which is the case for the techniques that involve reading signals from cells adhered on a plain gold substrate.

Supplementary Fig. 2 shows the optical DIC images of macrophage patterned on the gold microelectrodes after 21 h of cell culture for control cells with no LPS exposure (a) and cells treated with LPS at concentrations of (b) 0.1 μg/mL, (c) 1.0 μg/mL, and (d) 10 μg/mL. The control cells appeared small and round in shape, while LPS-treated cells underwent a morphological change and exhibited an enlarged, dendritic-like shape. This morphological change was likely associated with the synthesis of intracellular peptides and proteins induced by LPS. A similar observation has been reported by Saxena et al., when macrophage cells on a solid glass slide were cultured with LPS and exhibited an increased size and a transformation to dendritic-like morphology due to cell differentiation (Saxena et al., 2003).

3.1. Responses of microphage cells in singlet, doublet and triplet states to LPS

Cells in an isolated state (e.g., one cell on each microelectrode) generally respond differently to an external stimulus than when they are in a communicating state (e.g., a cluster of cells on a microelectrode). This is a topic of extensive study in cell biology and an important, but poorly understood issue in the development of cell-based sensors. To reveal this difference, macrophage cells were patterned in singlet, doublet, or triplet on

Table 1
The amide I wave number (cm^{-1}) of the single, double and triple cells before and after exposure to LPS at a concentration of 1 μg/mL

Sample	Single cell	Double cells	Triple cells
Control cells	1691 ± 1.2	1671 ± 2.5	1677 ± 3.2
LPS-exposed cells	1661 ± 1.6	1665 ± 2.6	1658 ± 3.4

gold electrodes of 10 μm × 10 μm by culturing cells with LPS. The top panel of Fig. 1 shows exemplary optical DIC images of cell morphology for these cell states, and the bottom panel shows the corresponding synchrotron IR spectra of the cells before and after exposure to LPS at a concentration of 1 μg/mL for 21 h.

Table 1 lists the characteristic wave numbers acquired from cells of the three different states before and after exposure to LPS, each averaged over four electrodes of the same state and expressed as mean ± S.D. cm^{-1}. Prior to exposure to LPS, cells in the singlet state have a characteristic amide I peak at 1691 ± 1.2 cm^{-1}, while cells in the doublet and triplet states have the characteristic peaks at 1671 ± 2.5 and 1677 ± 3.2 cm^{-1}, respectively.

The difference in amide I characteristic band between the three cell states, even before cells were exposed to LPS, suggests that the cell–cell interactions affect the IR signatures of cells. The degree of IR shifts after the cells were exposed to LPS also differed substantially among the three cell states with the cells in the singlet state exhibiting the greatest shift. Additionally, the cells in the singlet state yielded more consistent data than the other two, as characterized by its smallest standard deviation. The greater uncertainty in IR shifts produced by the cells in doublet and triplet states may be attributable to the interactions between cells in the cell clusters, and furthermore, such uncertainty was seen to increase with increased cell number in the cell cluster.

3.2. IR spectral changes of single macrophage cells induced by LPS at various concentrations

The left panel of Fig. 2 shows the synchrotron IR spectra of macrophage cells in singlet state after treated with LPS at different concentrations for 21 h. The right panel shows exemplary optical images of the cells from which the spectra were acquired. For both panels, (a) corresponds to the cell cultured without PLS (as control), and (b) through (d) correspond to the cells cultured with LPS at concentrations of 0.1, 1.0, and 10 μg/mL, respectively. Images in Fig. 2 show that all the LPS-treated cells exhibited dendritic morphology and expanded across the electrode as the LPS concentration increased. The change in IR signature is also dependent on the LPS concentration, characterized by the shifts of both amide I and amide II peaks of cell proteins.

The peak of amide I group (predominantly C=O stretching vibration of amide) shifted from 1691 ± 1.2 cm^{-1} before cell exposure to LPS, to 1676 ± 1.0 cm^{-1} (10 μg/mL LPS), 1661 ± 1.0 cm^{-1} (1 μg/mL LPS), and 1659 ± 1.7 cm^{-1} (0.1 μg/mL LPS) post-exposure. These peak shifts in wave number are presented as main ± standard deviation calculated from
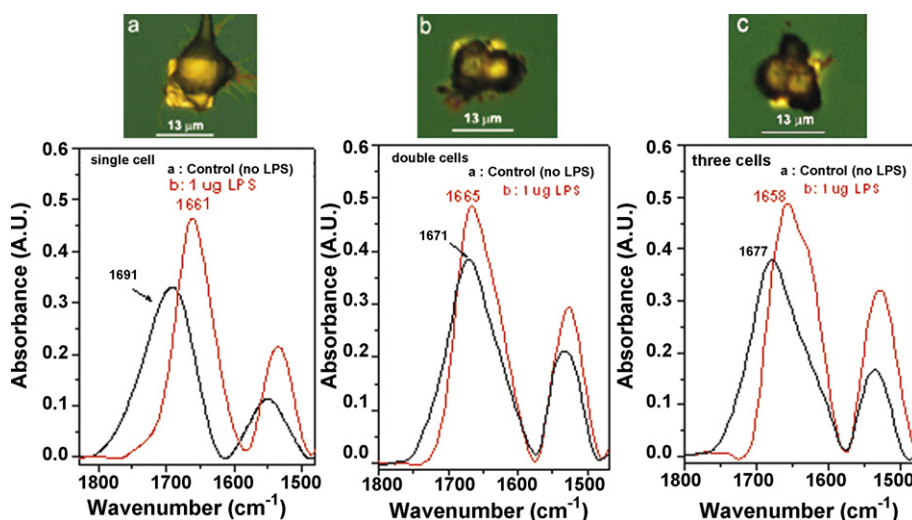
Fig. 1. (Top panel) Optical DIC images of 100 μm^2 electrodes hosting (a) a single macrophage cell, and (b) two cells, and (c) three cells, after treatment with 1 $\mu g/mL$ LPS for 21 h. (Bottom panel) Real-time synchrotron IR spectra of (a) a single cell, (b) double cells, and (c) triple cells before and after treatment with LPS.

eight electrodes of two substrates for each sample set. The characteristic peaks moved towards lower wave numbers initially with increased LPS concentration, but to higher wave numbers after reaching a minimum at LPS concentrations between 0.1 and 1.0 $\mu g/mL$. This peak reversion is believed to be due to cell death at high LPS concentrations.

To confirm this hypothesis, cellular viability was assessed by staining cells in singlet state with annexin V (green for apoptotic cells) and propidum iodide (red for necrotic cells) after they were exposed to LPS at concentrations of 0.1, 1.0 and 10 $\mu g/mL$, respectively. Fig. 3 shows exemplary images of cells treated with LPS at a concentration of 10 $\mu g/mL$, indicating that the cell underwent apoptosis and necrosis. Cellular viability was quantified in terms of ratios of apoptotic and necrotic cells to the total cells on 238 electrodes on duplicate substrates. The result indicated that cells treated with LPS at a concentration of 10 $\mu g/mL$ underwent 66.5% apoptosis (positive annexin V staining) and 41.1% necrosis (positive propidum iodide staining), respectively. Control cells and the cells treated with LPS at concentrations of 0.1 and 1.0 $\mu g/mL$ showed less than 8% apoptosis and no necrosis was identified. Images of cells treated with LPS at 0.1 and 1.0 $\mu g/mL$ are not shown in the figure due to absence of statistically significant fluorescence.

These experiments showed a LPS concentration-dependent response of single cells that can be readily detected by FTIR. It is worthwhile to note that a peak shift of 2–7 cm^{-1} in wave number has been used to identify diseased tissue from healthy tissues in multi-cell platforms (Miller et al., 2002; Wood et al., 1998). Here a shift in the order of a few tens of wave numbers (e.g., 30 cm^{-1} observed at LPS concentration of 1.0 $\mu g/mL$) demonstrated a high sensitivity of this single-cell-based platform. Such sensitivity may allow for identification of bacterium of very small concentration and sample volume. Furthermore, the degree of bacterium invasion (e.g., the percent of macrophage cells infected by LPS) can be assessed over a large number of sensing electrodes, and heterogeneous cellular behavior can be investigated with such a microarray of macrophages.

3.3. Time-dependent IR spectrum changes of single macrophage cells induced by LPS

Fig. 4 (left panel) shows IR spectra acquired by synchrotron-based FTIR microspectroscopy from single cells patterned on an array of gold microelectrodes before exposure to LPS as well as post-exposure to LPS at a concentration of 1 $\mu g/mL$ for (b) 3.5 and (c) 21 h, respectively. The optical images in Fig. 4 (right panel) show the corresponding cell morphology of the single macrophage cells on gold electrodes with a size of 100 μm^2 over the same time course. The morphology of the LPS-treated
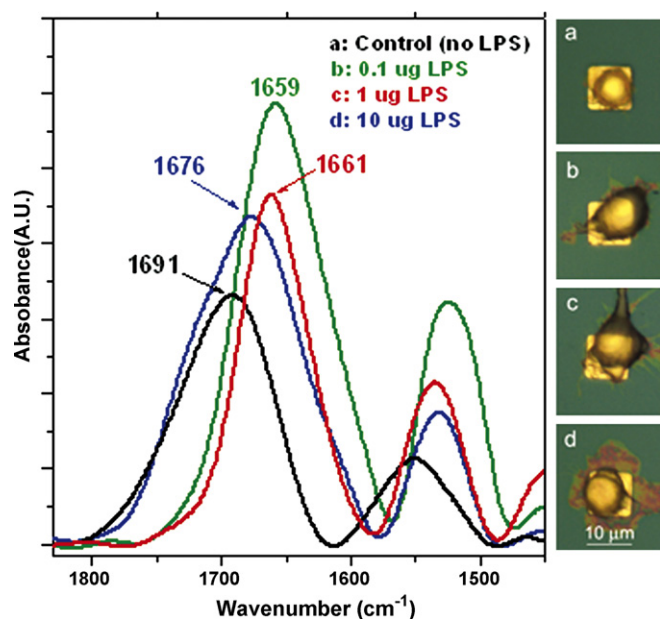
Fig. 2. (Left panel) Real-time synchrotron FTIR spectra taken from single macrophage cells patterned on gold electrodes with an area of 100 μm^2. (Right panel) Optical DIC images of macrophage cells. Cells were treated with (a) no LPS, and with LPS at concentrations of (b) 0.1 $\mu g/mL$, (c) 1.0 $\mu g/mL$, and (d) 10 $\mu g/mL$ for 21 h.
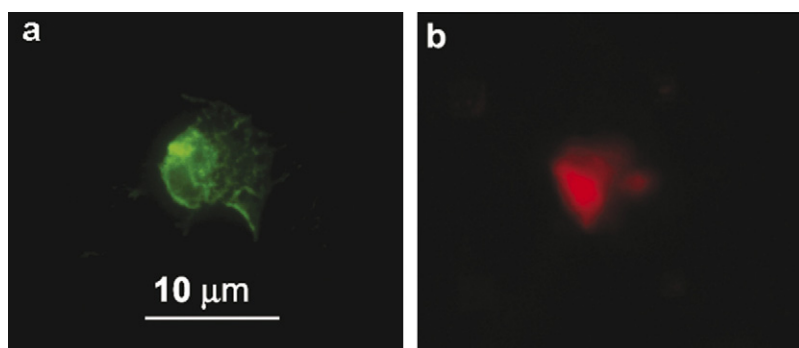
Fig. 3. Optical DIC images of a single macrophage cell patterned on a gold electrode with a surface area of 100 μm². The cell was cultured with 10 μg/mL LPS for 21 h and stained with Annexin V (a) and propidium iodide (b) for 15 min.

cell was seen to change with LPS exposure time, from a spherical shape to a dendritic shape with increased size over time. The change in IR spectrum over time during the LPS exposure is characterized by the continued shifts of both amide I and amide II peaks from high to low wave numbers and an increase in signal intensity. The IR shifts in amide I spectrum may indicate the change in protein structure as a result of upregulating various proteins and peptides involved in the macrophage activation cascade initiated by LPS. Hamilton et al., investigated biochemical events within macrophages in response to LPS and reported that LPS induced the synthesis of various polypeptides in the cells. Some peptides were short-lived (did not accumulate in LPS-treated cells) and played a regulatory role while others were long-lived (accumulated in LPS-treated cells) and played a functional role (Hamilton et al., 1986). Thus, the IR shift and the intensity increase for cells exposed to LPS for 3.5 h might be due to synthesis of short-lived peptides. The IR peak change for cells treated with LPS for 21 h might be attributable to the presence of long-lived polypeptides. The presence of a single peak for all the amide I bands in Fig. 4 suggests that proteins with α-helical secondary structure are dominant (Miller et al., 2002). The current experiment suggests that the variation in wave number in response to LPS invasion, as detected by the single-cell system

reported here, is adequate for identification of bacterium in a short period (hours here versus days by conventional bacterial detection methods).

3.4. Influence of electrode size and light source on detection sensitivity

IR signal intensity depends directly on the brightness of IR source and the size of the electrode that hosts the cell. In a gold-patterned silicon platform, the maximum signal intensity is obtained when the synchrotron IR focal point is at the center of the gold electrode and the noise from the silicon oxide background is minimized. The superior brightness of the synchrotron source with a spatial resolution less than 10 μm provides high sensitivity for detection of single cells on electrodes of 100 μm² as shown above. However, a conventional IR thermal source with an effective beam diameter of ∼75 μm requires electrodes larger than the beam size to reduce the signal loss to the surrounding area. To study the effect of electrode size on detection sensitivity and the possible use of conventional FTIR for bacterial detection with our single-cell system, FTIR spectra from single-cell arrays with electrode sizes of 25, 100, and 400 μm², respectively, were acquired using both synchrotron and conventional FTIR spectromicroscopy.

FTIR spectra shown in Fig. 5A and B were acquired by synchrotron and conventional FTIR, respectively. The signal intensity was seen to increase with increased electrode size for both systems. Characteristic peaks of cell membranes at wave numbers of 2800–3600 cm⁻¹ and cellular proteins at 1200–1700 cm⁻¹, are resolved well with the synchrotron source even for the smallest electrode size (25 μm²) (Fig. 5A). Though at a significantly lower signal intensity, the IR signals acquired with the conventional FTIR are well resolved for the 100 and 400 μm² microelectrodes (Fig. 5B). These results indicate that the current single-cell platform can be used with conventional FTIR spectromicroscopy if the electrode surface area is larger than 100 μm². It is noteworthy mentioning that although increasing electrode size will increase the signal intensity, it also increases the probability of adhesion of multiple cells on an electrode, rendering single-cell patterning more difficult. A comparison of the IR spectra acquired from cells on gold electrodes of different sizes reveals no identifiable difference in IR signature.
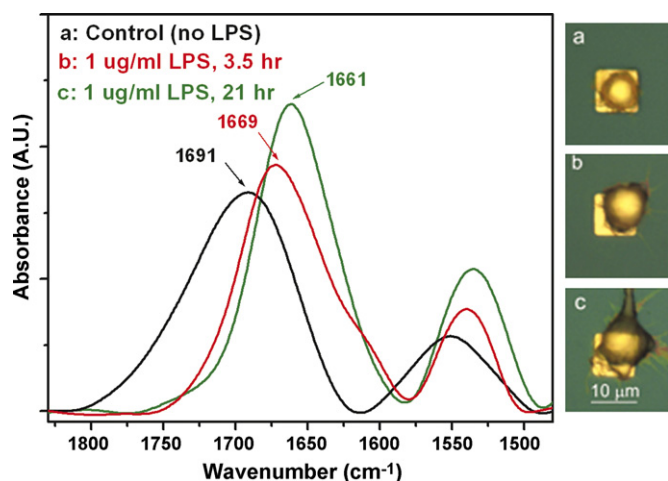
Fig. 4. Real-time synchrotron IR spectrum of a single cell response to LPS (1.0 μg/mL) over time.
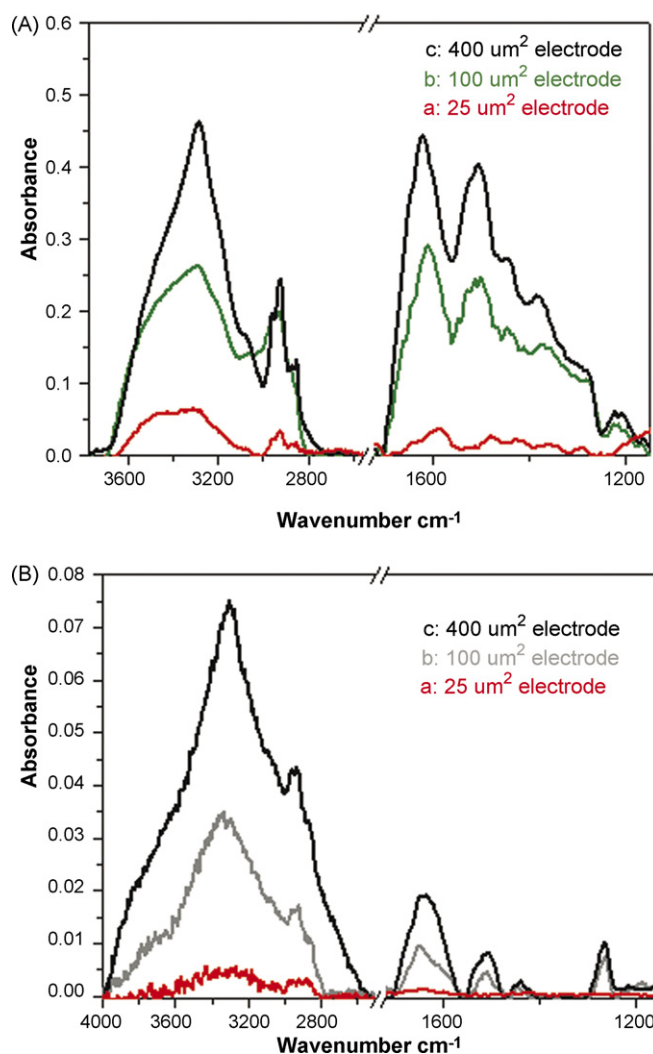
Fig. 5. FTIR spectra of single macrophage cells on electrodes of three different sizes, acquired by (A) synchrotron FTIR and (B) conventional FTIR (aperture size: $90 \mu m \times 90 \mu m$). In both A and B, the spectra were taken from electrodes of (a) $25 \mu m^2$, (b) $100 \mu m^2$, and (c) $400 \mu m^2$, respectively.

4. Conclusions

Microarrays of cell-based biosensors were fabricated by patterning macrophage cells on gold electrodes on silicon oxide substrates. Microarrays patterned with single cells respond differently to LPS than multi-cell arrays, and single-cell arrays were found to generate the most significant IR shifts upon exposure to LPS as compared to multi-cell systems and thus provide the highest detection sensitivity. Variations in IR spectrum for the single-cell system were found to be dependent on LPS concentration and the duration of cell exposure to LPS. This cell-based platform may potentially provide a time- and cost-effective means to detect and analyze bacterium invasion in a few hours as opposed to conventional bacterium detection technology in a few days. It may allow for large-scale, systematic studies of equally cultured macrophage cells and thus the statistical analysis over a large number of individual cells.

Appendix A. Supplementary data

Supplementary data associated with this article can be found, in the online version, at doi:10.1016/j.bios.2007.04.010.

References

Akashi, S., Shimazu, R., Ogata, H., Nagai, Y., Takeda, K., Kimoto, M., Miyake, K., 2000. J. Immunol. 164 (7), 3471–3475.

Andrews, W., 1992. FAO Food Nutr. Pap. 14 (4 Revis 1), 1–338.

Bashir, R., 2004. Adv. Drug Deliv. Rev. 56 (11), 1565–1586.

Carr, G.L., 2001. Rev. Sci. Instrum. 72 (3), 1613–1619.

Chiou, P.Y., Ohta, A.T., Wu, M.C., 2005. Nature 436 (7049), 370–372.

Cohen, J., 2002. Nature 420 (6917), 885–891.

Dumas, P., Jamin, N., Teillaud, J.L., Miller, L.M., Beccard, B., 2004. Faraday Discuss. 126, 289–302.

Elowitz, M.B., Levine, A.J., Siggia, E.D., Swain, P.S., 2002. Science 297 (5584), 1183–1186.

Frevel, M.A.E., Bakheet, T., Silva, A.M., Hissong, J.G., Khabar, K.S.A., Williams, B.R.G., 2003. Mol. Cell. Biol. 23 (2), 425–436.

Fujihara, M., Muroi, M., Tanamoto, K., Suzuki, T., Azuma, H., Ikeda, H., 2003. Pharmacol. Ther. 100 (2), 171–194.

Hamilton, T.A., Jansen, M.M., Somers, S.D., Adams, D.O., 1986. J. Cell. Physiol. 128 (1), 9–17.

Hyden, H., 1995. TRAC-Trends Anal. Chem. 14 (4), 148–154.

Kirkley, J.E., Thompson, B.J., Coon, J.S., 2003. Scand. J. Immunol. 58 (1), 51–58.

Lan, S., Veiseh, M., Zhang, M., 2005. Biosens. Bioelectron. 20 (9), 1697–1708.

Levinson, E., Lerch, P., Martin, M.C., 2006. Infrared Phys. Technol. 49, 45–52.

Lorenzelli, L., Margesin, B., Martinoia, S., Tedesco, M.T., Valle, M., 2003. Biosens. Bioelectron. 18 (5–6), 621–626.

Martin, M.C., McKinney, R.W., 1998. Proceed. Mater. Res. Soc. 524, 11–15.

Martin, M.C., McKinney, W.R., 2001. Ferroelectrics 249 (1–2), 1–10.

Miller, L.M., Dumas, P., Jamin, N., Teillaud, J.L., Miklossy, J., Forro, L., 2002. Rev. Sci. Instrum. 73 (3), 1357–1360.

Raetz, C.R.H., 1990. Annu. Rev. Biochem. 59, 129–170.

Rovida, E., Paccagnini, A., Del Rosso, M., Peschon, J., Dello Sbarba, P., 2001. J. Immunol. 166 (3), 1583–1589.

Saxena, R.K., Vallyathan, V., Lewis, D.M., 2003. J. Biosci. 28 (1), 129–134.

Schumann, R.R., Leong, S.R., Flaggs, G.W., Gray, P.W., Wright, S.D., Mathison, J.C., Tobias, P.S., Ulevitch, R.J., 1990. Science 249 (4975), 1429–1431.

Soler, C., Valdes, R., Garcia-Manteiga, J., Xaus, J., Comalada, M., Casado, F.J., Modolell, M., Nicholson, B., MacLeod, C., Felipe, A., Celada, A., Pastor-Anglada, M., 2001. J. Biol. Chem. 276 (32), 30043–30049.

Teruel, M.N., Meyer, T., 2002. Science 295 (5561), 1910–1912.

Triantafilou, M., Triantafilou, K., 2003. J. Endotoxin Res. 9 (5), 331–335.

Ulevitch, R.J., Tobias, P.S., 1995. Annu. Rev. Immunol. 13, 437–457.

van Bergen, A., Papanikolaou, T., Schuker, A., Moller, A., Schlosshauer, B., 2003. Brain Res. Protoc. 11 (2), 123–133.

Veiseh, M., Zhang, M., 2006. J. Am. Chem. Soc. 128 (4), 1197–1203.

Veiseh, M., Zareie, M.H., Zhang, M.Q., 2002. Langmuir 18 (17), 6671–6678.

Wang, X.B., Li, M., 2003. Assay Drug Dev. Technol. 1 (5), 695–708.

Wiklund, N.P., Iversen, H.H., Leone, A.M., Cellek, S., Brundin, L., Gustafsson, L.E., Moncada, S., 1999. Acta Physiol. Scand. 167 (2), 161–166.

Wood, B.R., Quinn, M.A., Tait, B., Ashdown, M., Hislop, T., Romeo, M., McNaughton, D., 1998. Biospectroscopy 4 (2), 75–91.

Yang, M., Prasad, S., Zhang, X., Morgan, A., Ozkan, M., Ozkan, C.S., 2003. Sens. Mater. 15 (6), 313–333.

Zhang, H.W., Peterson, J.W., Niesel, D.W., Klimpel, G.R., 1997. J. Immunol. 159 (10), 4868–4878.